

# Electrochemical Heteroarylation and Amidation of Alkanes using Activated Glassy Carbon Electrodes without Mediators

Loris Laze, Jose C. Gonzalez-Gomez,\* Irene Bosque\*

*Instituto de Síntesis Orgánica (ISO) and Departamento de Química Orgánica  
Universidad de Alicante, Apdo. 99, 03080 Alicante, Spain*

## Abstract

The functionalization of challenging unactivated C(sp<sup>3</sup>)-H bonds was achieved electrocatalytically *via* hydrogen atom transfer and without mediators. This was possible through the sole activation of the surface of the Glassy Carbon Electrode in an electrochemical fashion using a phosphate buffer. This activation produced oxygenated functional groups on the surface, capable of abstracting these hydrogen atoms from C(sp<sup>3</sup>)-H of alkanes. Minisci and Ritter-type reactions were achieved using this procedure. Extensive characterization of the AGCE and preliminary mechanistic studies allow us to propose plausible reaction mechanisms. Furthermore, a regular battery can be used within this protocol to achieve the desired substituted alkanes under inexpensive and user-friendly conditions.

## Keywords

Minisci reaction, Ritter reaction, Activated Glassy Carbon Electrode, electrocatalysis, C-H functionalization

## Introduction

Aliphatic compounds are important and ubiquitous, playing a crucial role in many industries, such as pharmaceutical and agrochemical. For this reason, the selective modification of these structures has attracted the attention of synthetic chemists. There are several strategies to transform aliphatic compounds, activating the C(sp<sup>3</sup>)-H bonds being the most direct, selective, and desirable. However, the strength of unactivated C(sp<sup>3</sup>)-H bonds (BDE (cyclohexane) = 99 kcal/mol)<sup>1</sup> makes this functionalization often challenging.

Chemists have dealt with this problem in many different ways (Figure 1), from the classic intramolecular Hofmann–Löffler–Freitag reaction<sup>2</sup> or metal-catalyzed strategies using directing groups<sup>3</sup> to heterogeneous photocatalytic activation using semiconductors<sup>4</sup> (Figure 1A-C). Among them, catalytic and tunable hydrogen atom transfer (HAT) agents have emerged to homolytically break different C-H bonds to generate the C-centered radical in the last few decades.<sup>5</sup> In this regard, we recently described a photocatalyzed strategy to perform Minisci-type reactions using pyridine *N*-oxides as HAT species (BDE (PyO-H), 99 kcal/mol), which effectively abstracted a hydrogen atom from a variety of alkanes, ethers, and amides among others.<sup>6</sup> Following our interest in the Minisci reaction and developing more sustainable methodologies, we sought to investigate electrocatalysis in this oxidative cross-dehydrogenative coupling (CDC), which would avoid the addition of any external chemical oxidant and the formation of chemical waste (Figure 1D). Due to the greenness of the process, electrochemical oxidation methods to achieve C-H bond activations have attracted much attention in the last decade,<sup>7–11</sup> especially when combined with metal catalysis<sup>12,13</sup> or non-metallic HAT agents, such as sulfate anion<sup>14</sup> or iodine,<sup>15</sup> among others. In this context, a recent work utilized sulfuric acid as a source of sulfate radical anion after anodic oxidation.<sup>16</sup> This method allowed the electrocatalytic Ritter-type amination of a broad range of alkanes. However, sulfuric acid is a redox mediator that is too aggressive to scale up the reaction, and milder conditions are desired.

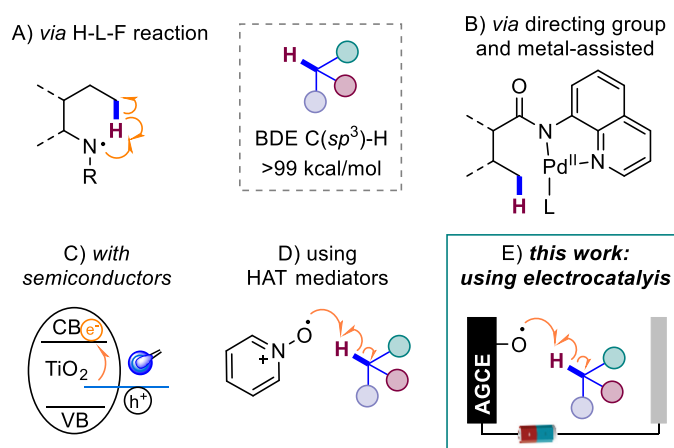


**Figure 1:** Selected strategies for the activation of C(*sp*<sup>3</sup>)-H bonds

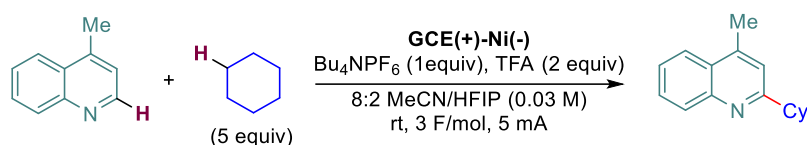
Less studied in synthetic chemistry is the activation of the electrode surface area to achieve improved reactivity.<sup>17,18</sup> This is a much simpler approach but often as effective as the most complicated dual catalytic cycle and still much more convenient and cost-effective. Recent electrochemical reports show potential for the desired catalytic activity. However, the applications in bulk reactions of these

activated electrodes are often rare. This is the case of glassy carbon electrodes (GCE).<sup>19</sup> This material has remarkable electrocatalytic properties at a relatively low cost, considering that electrodes are usually reused in electrocatalytic reactions. Activated glassy carbon electrodes (AGCE) have been reported through several methods, from vacuum heating<sup>20</sup> or ultrasonication<sup>21</sup> to preanodization.<sup>22</sup> However, these activations have rarely been applied to organic synthesis. This work describes our efforts in the Minisci-type alkylation of azaarenes with alkanes and the Ritter reaction between alkanes and nitriles using an AGCE (Figure 1E). Remarkably, *the electrochemical activation of the electrode is with a phosphate buffer, without requiring any sacrificial reagent, under very mild and sustainable conditions.*

## Results and Discussion

Lepidine and cyclohexane were selected as model substrates. Using TFA (2 equiv), Bu<sub>4</sub>NPF<sub>6</sub> as supporting electrolyte (SE, 1 equiv) in a mixture of acetonitrile and 1,1,1,3,3,3-hexafluoroisopropanol (HFIP, 8:2, 0.03 M) the reaction was run with a Glassy Carbon Electrode (GCE) as anode and Nickel as cathode, at 5 mA (total charge of 3 F/mol) at room temperature. Under these conditions, the desired product was obtained in low yield (Table 1, entry 1). Following our previous work, we decided to test different pyridine *N*-oxides as HAT (Table S1), obtaining a higher yield in the presence of 30 mol% of 2,4,6-collidine *N*-oxide (**HAT3**), but still insufficient (entry 2). Different electrodes were tested as anode and cathode (Table S2), which provided poorer yields. We decided to explore heterogeneous catalysis by anchoring 2,6-dimethylpyridine on the GCE. The oxidation of the anchored pyridine was conducted by submerging the electrode in an MCPBA solution overnight, mimicking the structure of **HAT3**. The reaction using this **GCE-HAT3** anchored electrode provided a slightly better yield (entry 3). Surprisingly, the control reaction performing the overnight MCPBA-mediated oxidation of the bare GCE in the absence of the anchored pyridine-*N*-oxide gave a significantly higher reaction yield, obtaining 80% of the expected product (entry 4) and complete conversion by increasing the total charge (entry 5), suggesting that the oxidated area of the GCE is a better HAT mediator than **HAT3**. We tested a more environmentally friendly oxidation of the GCE using a phosphate buffer (NaH<sub>2</sub>PO<sub>4</sub> and Na<sub>2</sub>HPO<sub>4</sub> (pH 7, 0.1 M)).<sup>23</sup> The number of scans needed to activate the electrode was further optimized (Table S4). Using the optimal activation method, the modified electrode (AGCE) yielded 85% of product 1 under standard reaction conditions, which rose to 94% when the amount of cyclohexane was increased (entry 7). Importantly, the control reaction without current gave complete recovery of the lepidine (entry 8).

### Table 1. Optimization of the model reaction



| Entry    | Deviation from above                           | Yield of <b>1</b> (%) <sup>a</sup> |
|----------|--|------------------------------------|
| <b>1</b> | No deviation                                   | 36                                 |
| <b>2</b> | <b>HAT3</b> <sup>b</sup> (30 mol%) in solution | 40                                 |
| <b>3</b> | GCE- <b>HAT3</b> anchored <sup>c,d</sup>       | 50                                 |
| <b>4</b> | GCE <sup>d</sup>                               | 80                                 |
| <b>5</b> | GCE, <sup>d</sup> 5 F/mol                      | 100                                |
| <b>6</b> | AGCE, <sup>e</sup> 5 F/mol                     | 85                                 |
| <b>7</b> | AGCE, <sup>e</sup> 5 F/mol, 10 equiv CyH       | <b>94</b>                          |
| <b>8</b> | No current                                     | 0                                  |

Reactions were performed on a scale of 0.25 mmol of lepidine. <sup>a</sup>GC yield based on remaining SM without calibration. <sup>b</sup>**HAT3**: 2,4,6-collidine *N*-oxide. <sup>c</sup>GCE-**HAT3**: glassy carbon electrode anchored with 2,6-lutidine. <sup>d</sup> Electrode activated with MCPBA overnight. <sup>e</sup>AGCE: activated glassy carbon electrode using phosphate buffer.

### Substrate scope

Having found the optimal conditions, we approached the substrate scope by examining different azaarenes in the reaction with cyclohexane as the  $C(sp^3)$ -H coupling partner (Figure 2). Quinolines with substituents placed at C4 reacted better than the C2 substituted, obtaining C2 or C4 cyclohexyl derivatives (products **1-5**) from moderate to good yields (36-82%). Unsubstituted quinoline and 3-methylquinoline were converted into inseparable mixtures of C2- and di-alkylated products at C2/C4 (**6**) and C4- and C2- alkylated products at C2/C4 (**7**), respectively. Halides groups (-Cl,-Br) in different positions of quinolines gave the desired products (**8-11**) in moderate yields. We also explored the reaction with a nitro group as an electron-withdrawing group, obtaining the corresponding product (**12**) in good yield. Other azaarenes, such as 2,2'-biquinoline and phenanthridine, were suitable substrates for the reaction, giving moderate yields of the corresponding alkylated products (**13, 14**). Interestingly, our protocol was applied to functionalize the natural cinchonine, giving **15** in a 35% yield. Different C-H partners were also evaluated. Cycloalkanes reacted to provide the desired products (**16-19**) from moderate to good yields. The bridged alkane norbornane was successfully converted into the desired exo product **20** with excellent *endo/exo* selectivity. Interestingly, dioxane reacted smoothly, giving the desired product **21** in 38% yield, and the reaction using pivalaldehyde provided the alkylated product (**22**) after decarbonylation. Finally, adamantane and other derivatives were also tested, giving the desired products (**23-25**) in moderate yields. Interestingly, in all three cases, the stronger C-H bond of the adamantane (BDE(C1-H) 99 kcal/mol vs. BDE(C2-H) 96

kcal/mol)<sup>24</sup> was alkylated preferentially. This results from an enhanced polar effect at C1-H due to the positively charged surface of the anode. Presumably, there is an increased charge-transfer character in the transition state since a positive charge is developed at the C of the adamantane through the HAT process, a charge that is more stable at the tertiary C1 than at the secondary C2. The same phenomena can explain the high selectivity observed in product **25**, where the weaker secondary and tertiary Csp<sup>3</sup>-H bonds of the side chain were untouched.

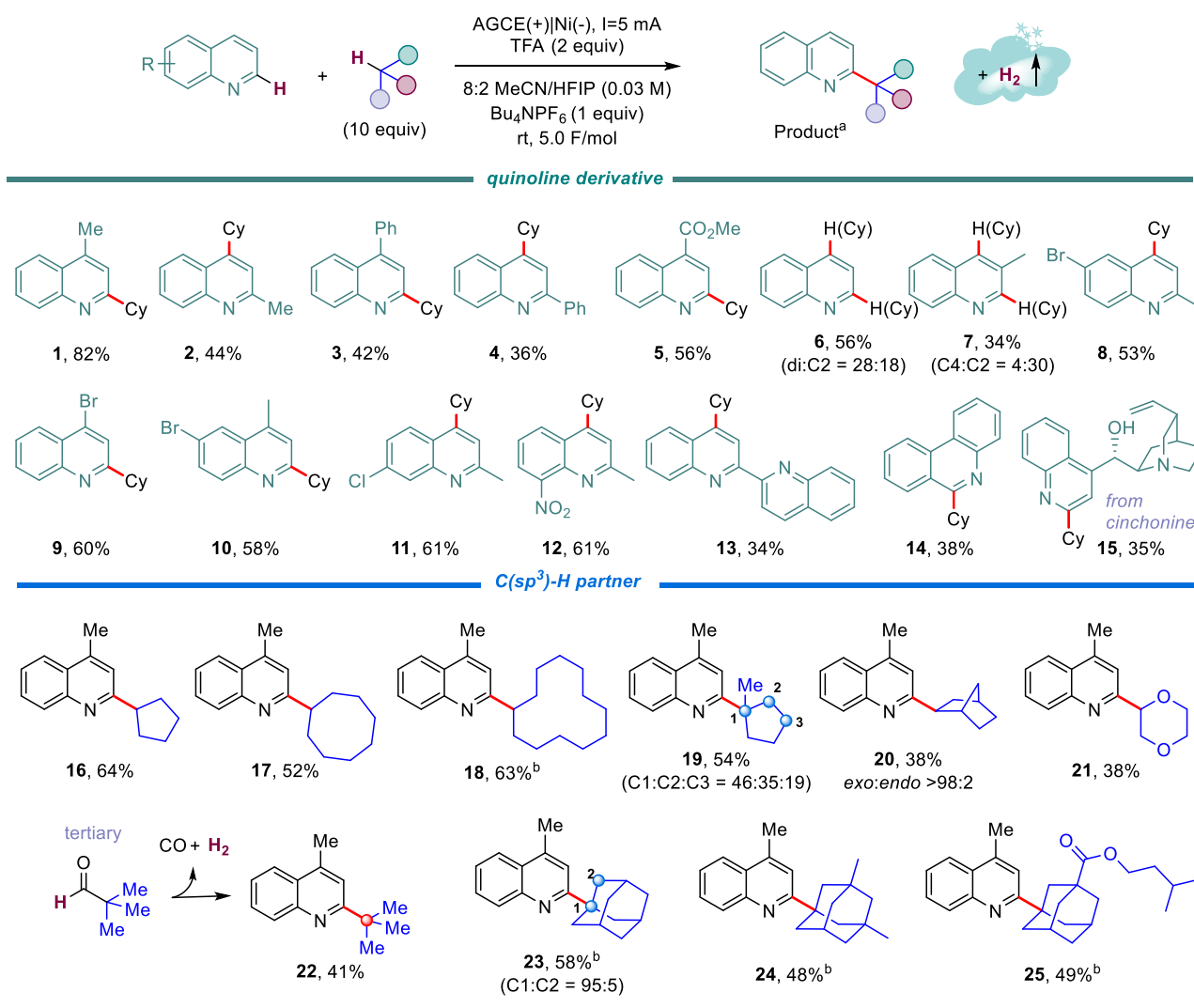


**Figure 2:** Substrate scope for the Minisci-type reaction. Reaction conditions: Quinoline (0.25 mmol), R-H (2.5 mmol), SE (1 equiv), TFA (2 equiv) 8:2 MeCN:HFIP (8 mL). All reagents were added in open-air conditions. After complete dissolution, the electrodes were placed in the reaction media, the vial closed, and the current was circulated (5 mA, 5.0 F/mol). <sup>a</sup>Yields for isolated pure products are given. <sup>b</sup> 5 equiv R-H.

While performing the scope of the Minisci reaction, we observed by GC-MS the formation of a lighter product in large amounts in some cases. For instance, when adamantane was used, apart from the formation of the Minisci product, a new peak with high intensity and with *m/q* of 193 was detected. It is worth noting that an excess of adamantane was needed for the Minisci reaction, so this was not affected by the formation of the byproduct. After carefully analyzing the fragmentation pattern, we

realized it matched *N*-(adamant-1-yl)acetamide. Indeed, when we performed the reaction without lepidine using adamantane as a limiting reagent, complete conversion to the *N*-(adamant-1-yl)acetamide **26** was observed. Interestingly, high selectivity was again found towards C1 due to the enhanced polar effect previously commented on. This Ritter-type reaction demonstrated that reactions that proceed through a different mechanistic pathway were also possible using the AGCE. In literature, Ritter-type reactions have been performed under electrochemical conditions.<sup>16,25,26</sup> However, to our knowledge, this is the first one functionalizing an unactivated C(*sp*<sup>3</sup>)-H bond directly using the electrode and without a HAT mediator. Thus, we became interested in this new opportunity and tried to reoptimize the reaction conditions for this reaction (Table S3). After optimization, using 2.5 F/mol at 10 mA provided full conversion in shorter reaction times, and using a simpler SE such as LiClO<sub>4</sub> facilitated the isolation of the different products.

Having found the optimal conditions, we approached the substrate scope by first examining different adamantanes with acetonitrile as a nitrile source (Figure 3). Adamantane and 1,3-dimethyladamantane gave good yields (products **26** and **27**, 84% and 67%, respectively). We also explored the reaction with the isopentyl-adamantane-1-carboxylate, obtaining the corresponding product (**28**) in good yield (76%). Interestingly, this reaction was again completely selective to the C1 of the adamantane, even in the presence of weaker C-H bonds present at the open side chain, such as the secondary methylene in  $\alpha$ -position to the oxygen atom or the tertiary methine. Furthermore, our protocol was successfully applied when using adamantane in the presence of isobutyronitrile as a nitrile source, giving the desired product (**29**) in moderate yield. Cycloheptane and cyclooctane were also suitable substrates for the reaction in the presence of acetonitrile, giving products **30** and **31** in moderate yields (57% and 60%). Finally, indane was tested, providing the desired acetamide **32** in 44% yield (Figure 3).

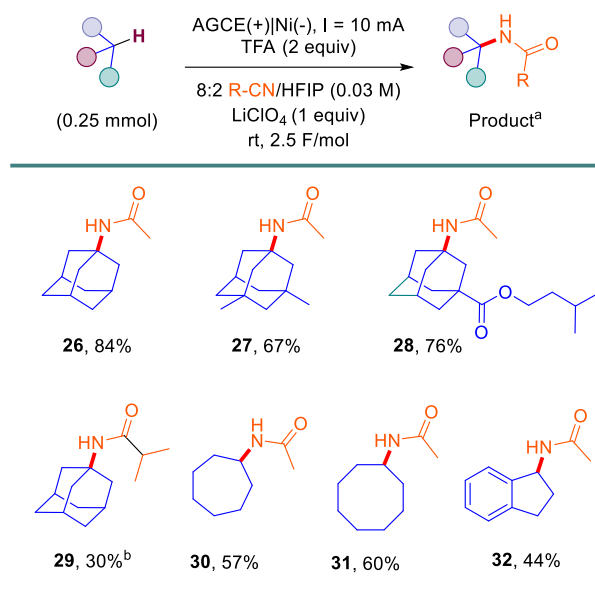


**Figure 3:** Scope for the Ritter-type amidation. Reaction conditions: C-H (0.25 mmol), SE (1 equiv), TFA (2 equiv), 8:2 MeCN:HFIP (8 mL). All reagents were added in open-air conditions. After complete dissolution, the electrodes were placed in the reaction media, the vial closed, and the current was circulated (10 mA, 2.5 F/mol). <sup>a</sup>Yields for isolated pure products are given. <sup>b</sup>Isobutyronitrile as nitrile source.

### AGCE analysis

To better understand the mechanism allowing for this alkane activation in the absence of any HAT mediator, a series of analyses were performed on the surface of the AGCE, and these results were compared with the surface of polished GCE. The activation of the GCE to obtain AGCE was monitored by CV, observing the appearance of a new oxidation and reduction peak couple, which is attributed to the generation of quinone/hydroquinone structure on the surface (Figure S2). A wettability test was also conducted, adding 10  $\mu\text{L}$  of water to the GCE and the AGCE (Figure 4A) and observing that the water slips easier on the AGCE than on the GCE, indicating the presence of a more hydrophilic surface on the AGCE. IR analysis (Figure S4) revealed a broad signal at  $>3000 \text{ cm}^{-1}$ , suggesting the presence of hydroxyl groups on the surface of the AGCE. Furthermore, XPS analysis of the surface of the AGCE revealed a higher content of O 1s on its surface compared to the GCE surface, where the only significant peak belongs to the C 1s (Figures 4B and S5). Indeed, analyzing the distribution of the C 1s in the AGCE, a substantial increase of the C=O and C-O groups is detected compared to the GCE, combined with a decrease in the C-C and C=C groups (Figures 4C, 4D, and S6). Raman spectroscopy performed on both surfaces (Figure 4E) showed a calculated I(D/G) ratio of 1.39 and 1.36 for the GCE and the AGCE, respectively, which indicates the dominance of  $sp^2$ -bonded carbons (see Figure S7 for further details). Finally, SEM images and EDX analysis were performed (Figures S8-S10). The GCE showed a 100% composition of C atoms (Figures 4F-G), while the AGCE showed an average of 28% of O atoms on the surface (Figures 4H-I). All these results



indicate that the buffer treatment can generate oxygenated functional groups on the surface of the GCE, activating the surface toward possible HAT processes.

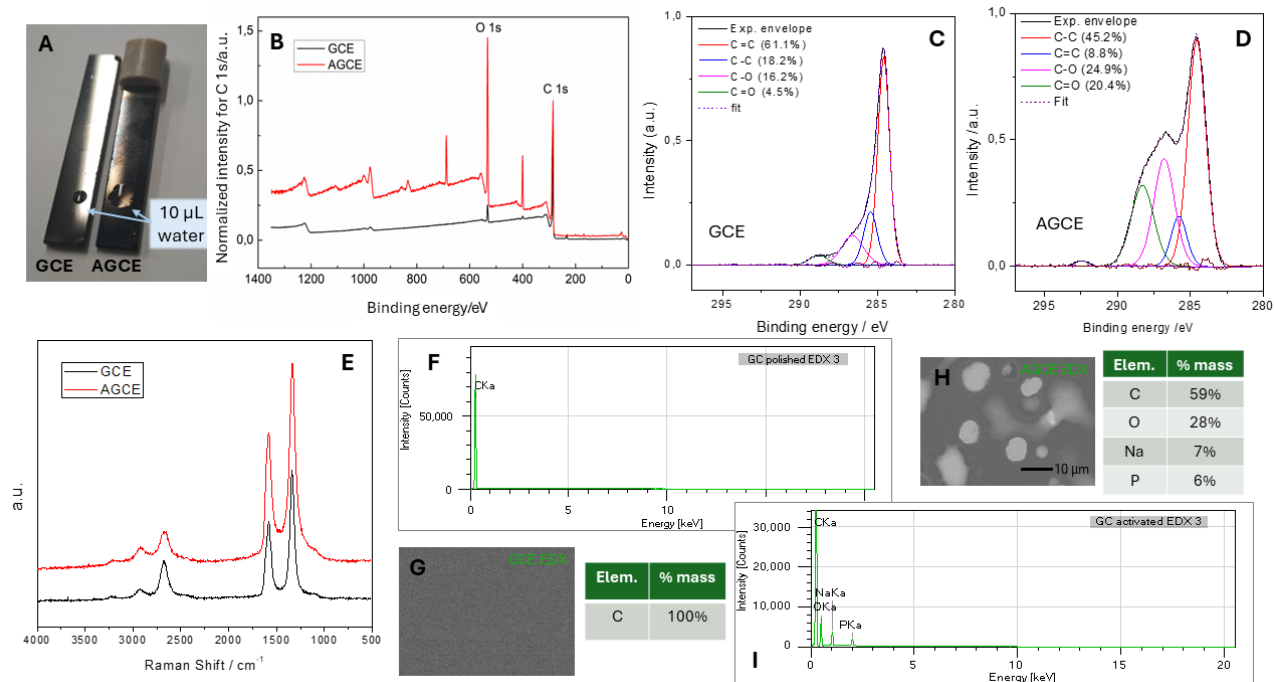


**Figure 4:** A: visual observation of wettability change between the GCE and AGCE after adding 10  $\mu\text{L}$  of water. B: XPS survey. C: XPS for C 1s at the GCE. D: XPS for C 1s at the AGCE. E: Raman spectra for GCE and AGCE. F and G: SEM and EDX analysis of the surface of GCE. H and I: SEM and EDX analysis of the surface of GCE.

## Mechanistic insights and reaction mechanism proposal

Mechanistic studies were conducted to gain a better understanding of the mechanistic pathways. To confirm the formation of the alkyl radical during the reaction,  $\beta$ -pinene was added to the reaction of lepidine with cyclohexane, observing the formation of the  $\beta$ -pinene-cyclohexane adduct and confirming the formation of the cyclohexyl radical (Figures 5A and S13). The addition of TEMPO or 1,1-diphenylethylene (radical scavengers) gave no formation of the corresponding Minisci product, as well as the addition of  $\text{CuCl}_2$ , a well-known single electron scavenger (Figures 5A, S11 and S2). The electrode analysis and the mechanistic studies allowed us to draw plausible mechanisms for these reactions (Figure 5B). The formation of an oxygen-centered radical on the surface of the AGCE after electrochemical oxidation promotes the HAT from the alkane, producing the corresponding alkyl radical. In the Minisci reaction, this alkyl radical is trapped by the protonated azaarene which, after deprotonation, gives the corresponding radical intermediate that suffers a second oxidation on the surface of the electrode, giving the corresponding product after a second deprotonation. On the other hand, the alkyl radical can also be further oxidized on the surface of the AGCE, forming the corresponding alkyl cation. A nucleophilic media, such as MeCN, promotes the Ritter amidation,



furnishing the corresponding acetamides after hydration. It is worth noting that for the Minisci reaction, a smaller current intensity was necessary to avoid overoxidation of the formed radical. In contrast, a higher intensity is allowed to perform the Ritter reaction since the alkyl radical must be further oxidized on the surface of the electrode.

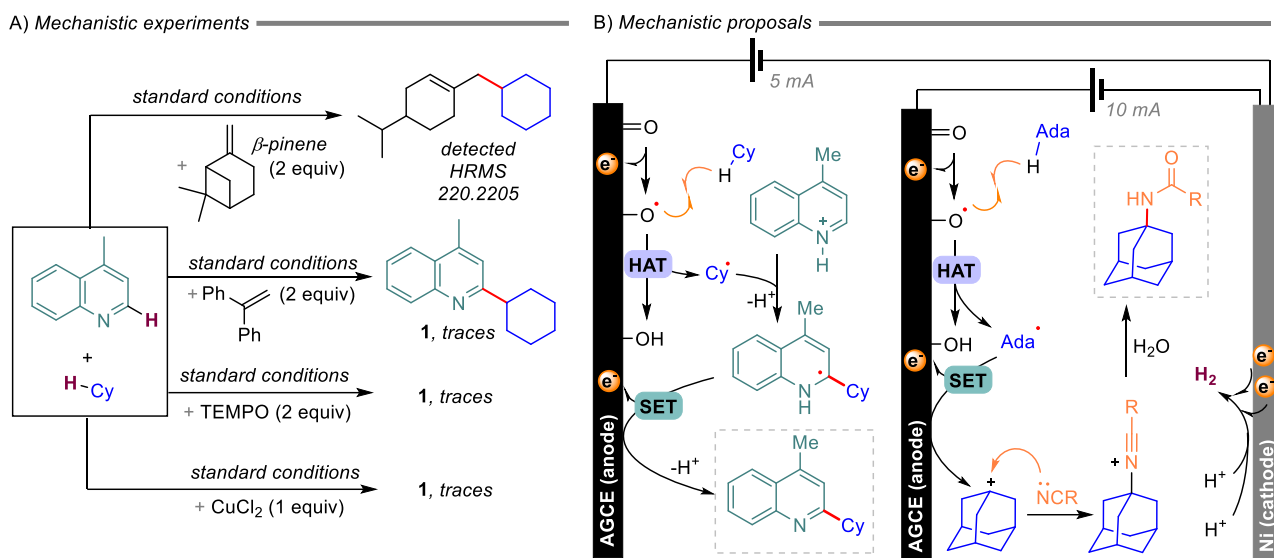


**Figure 5:** A: Mechanistic experiments adding different scavengers. B: Mechanistic proposals for the Minisci (left) and the Ritter (right) reactions.

To further demonstrate the utility of this procedure, a scale-up of the Minisci-type reaction was performed at 1.5 mmol-scale, giving an even better yield than when 0.25 mmol-scale was used (68% vs 48%, Figures 6A and S14). Moreover, since this is an electrocatalytic procedure, we tested both the Minisci and the Ritter-type reactions using a series of 1.5 V batteries (3 X 1.5 V were measured to have a voltage of ~4.0 V; see Figures S15-16 for further details), obtaining comparable results to the yields achieved using controlled current intensity. This experiment highlights the robustness and simplicity of this reaction, which can be performed using a regular battery.

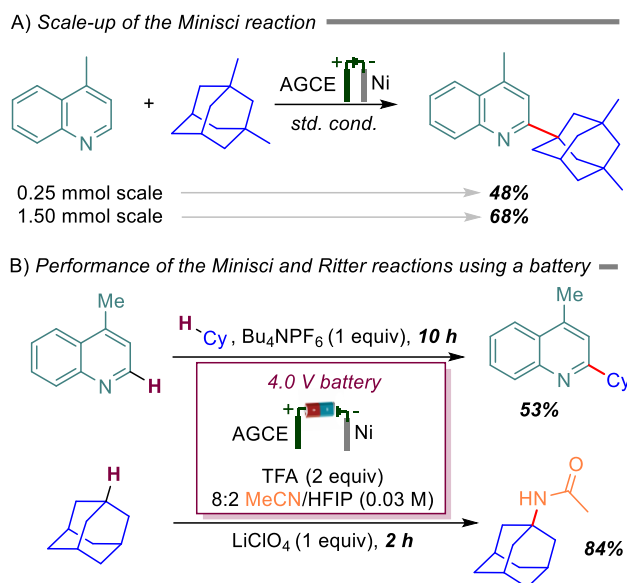


**Figure 6:** A) Scale-up of the Minisci-type reaction. B) Use of a 4.0 V battery in the Minisci and Ritter-type reactions.

## Conclusions

In summary, we have developed a simple electrocatalyzed protocol for functionalizing unactivated C( $sp^3$ )-H bonds by only using an AGCE as “HAT promoter” and electrode. The formed alkyl radicals were coupled with a variety of azaarenes in a Minisci cross-dehydrogenative coupling (CDC) reaction or further oxidized to being trapped with nitriles in a Ritter-type fashion. Furthermore, the method's robustness was tested by scaling up the reaction and using a simple battery as an electrical source, obtaining similar or improved results. This AGCE was activated under very mild electrochemical conditions using a phosphate buffer and characterized by several techniques, including XPS or EDX. Mechanistic studies confirmed the presence of radicals, and plausible mechanisms were proposed accordingly.

## AUTHOR INFORMATION

### Corresponding Author

\* Jose C. Gonzalez-Gomez

Instituto de Síntesis Orgánica (ISO) and Departamento de Química Orgánica Universidad de Alicante, 03080 Alicante (Spain); orcid.org/0000-0001-5334-7938; E-mail: josecarlos.gonzalez@ua.

\* Irene Bosque

Instituto de Síntesis Orgánica (ISO) and Departamento de Química Orgánica Universidad de Alicante, 03080 Alicante (Spain); orcid.org/0000-0003-0321-2167; Email: irene.bosque@ua.es

## Acknowledgments

This work was financially supported by the Generalitat Valenciana (CIAICO/2022/017 and SEJIGENT/2021/005). We thank MCIN/AEI and the “European Union NextGenerationEU” for the Grant “Consolidación Investigadora” (CNS2022-135161). We also thank Prof. Teresa Lana-Villareal from the Universidad de Alicante for the Raman spectroscopy measurements.

## References

- (1) Luo, Y. R. *Comprehensive Handbook of Chemical Bond Energies*; CRC Press, 2007.
- (2) Hofmann-Löffler-Freytag Reaction. In *Name Reactions in Organic Synthesis*; Parikh, A., Parikh, H., Parikh, K., Eds.; Foundation Books, 2006; pp 549–552. <https://doi.org/DOI:10.1017/UPO9788175968295.153>.
- (3) Das, J.; Ali, W.; Maiti, D. The Evolution of Directing Group Strategies for C(Sp)<sup>3</sup>–H Activation. *Trends in Chem.* **2023**, *5* (7), 551–560. <https://doi.org/10.1016/j.trechm.2023.05.003>.
- (4) Chai, Z. Heterogeneous Photocatalytic Strategies for C(Sp)<sup>3</sup>–H Activation. *Angew. Chem. Int. Ed.* **2024**, *63* (13), e202316444. <https://doi.org/https://doi.org/10.1002/anie.202316444>.
- (5) Matsumoto, A.; Maruoka, K. Design of Organic Radical Cations as Potent Hydrogen-Atom Transfer Catalysts for C–H Functionalization. *Asian J. Org. Chem.* **2024**, *13* (4), e202300580. <https://doi.org/https://doi.org/10.1002/ajoc.202300580>.
- (6) Laze, L.; Quevedo-Flores, B.; Bosque, I.; Gonzalez-Gomez, J. C. Alkanes in Minisci-Type Reaction under Photocatalytic Conditions with Hydrogen Evolution. *Org. Lett.* **2023**, *25* (48), 8541–8546. <https://doi.org/10.1021/acs.orglett.3c02619>.
- (7) Gao, X.; Wang, P.; Zeng, L.; Tang, S.; Lei, A. Cobalt(II)-Catalyzed Electrooxidative C–H Amination of Arenes with Alkylamines. *J. Am. Chem. Soc.* **2018**, *140* (12), 4195–4199. <https://doi.org/10.1021/jacs.7b13049>.
- (8) Yang, Q.-L.; Wang, X.-Y.; Lu, J.-Y.; Zhang, L.-P.; Fang, P.; Mei, T.-S. Copper-Catalyzed Electrochemical C–H Amination of Arenes with Secondary Amines. *J. Am. Chem. Soc.* **2018**, *140* (36), 11487–11494. <https://doi.org/10.1021/jacs.8b07380>.
- (9) Yang, Q.-L.; Wang, X.-Y.; Lu, J.-Y.; Zhang, L.-P.; Fang, P.; Mei, T.-S. Copper-Catalyzed Electrochemical C–H Amination of Arenes with Secondary Amines. *J. Am. Chem. Soc.* **2018**, *140* (36), 11487–11494. <https://doi.org/10.1021/jacs.8b07380>.
- (10) Huang, H.; Strater, Z. M.; Rauch, M.; Shee, J.; Sisto, T. J.; Nuckolls, C.; Lambert, T. H. Electrophotocatalysis with a Trisaminocyclopropenium Radical Dication. *Angew. Chem. Int. Ed.* **2019**, *58* (38), 13318–13322. <https://doi.org/https://doi.org/10.1002/anie.201906381>.
- (11) Strelakova, S.; Kononov, A.; Rizvanov, I.; Budnikova, Y. Acetonitrile and Benzonitrile as Versatile Amino Sources in Copper-Catalyzed Mild Electrochemical C–H Amidation Reactions. *RSC Adv* **2021**, *11* (59), 37540–37543. <https://doi.org/10.1039/D1RA07650G>.
- (12) Ma, C.; Fang, P.; Mei, T.-S. Recent Advances in C–H Functionalization Using Electrochemical Transition Metal Catalysis. *ACS Catal* **2018**, *8* (8), 7179–7189. <https://doi.org/10.1021/acscatal.8b01697>.

- (13) Sauermann, N.; Mei, R.; Ackermann, L. Electrochemical C–H Amination by Cobalt Catalysis in a Renewable Solvent. *Angew. Chem. Int. Ed.* **2018**, *57* (18), 5090–5094. <https://doi.org/10.1002/anie.201802206>.
- (14) Fu, Y.; Zhang, L.; Sun, M.; Cao, L.; Yang, L.; Cheng, R.; Ma, Y.; Ye, J. Direct Electrochemical Ritter-Type Amination of Electron-Deficient Arenes. *Eur. J. Org. Chem.* **2023**, *26* (35), e202300553. <https://doi.org/10.1002/ejoc.202300553>.
- (15) Liu, K.; Song, C.; Lei, A. Recent Advances in Iodine Mediated Electrochemical Oxidative Cross-Coupling. *Org. Biomol. Chem.* **2018**, *16* (14), 2375–2387. <https://doi.org/10.1039/C8OB00063H>.
- (16) Zhang, L.; Fu, Y.; Shen, Y.; Liu, C.; Sun, M.; Cheng, R.; Zhu, W.; Qian, X.; Ma, Y.; Ye, J. Ritter-Type Amination of C(sp<sup>3</sup>)-H Bonds Enabled by Electrochemistry with SO<sub>4</sub><sup>2-</sup>. *Nat. Comm.* **2022**, *13* (1), 4138. <https://doi.org/10.1038/s41467-022-31813-3>.
- (17) Fang, M.; Engelhard, M. H.; Zhu, Z.; Helm, M. L.; Roberts, J. A. S. Electrodeposition from Acidic Solutions of Nickel Bis(Benzenedithiolate) Produces a Hydrogen-Evolving Ni–S Film on Glassy Carbon. *ACS Catal* **2014**, *4* (1), 90–98. <https://doi.org/10.1021/cs400675u>.
- (18) Gorlin, Y.; Chung, C.-J.; Nordlund, D.; Clemens, B. M.; Jaramillo, T. F. Mn<sub>3</sub>O<sub>4</sub> Supported on Glassy Carbon: An Active Non-Precious Metal Catalyst for the Oxygen Reduction Reaction. *ACS Catal* **2012**, *2* (12), 2687–2694. <https://doi.org/10.1021/cs3004352>.
- (19) JENKINS, G. M.; KAWAMURA, K. Structure of Glassy Carbon. *Nature* **1971**, *231* (5299), 175–176. <https://doi.org/10.1038/231175a0>.
- (20) Fagan, D. T.; Hu, I. Feng.; Kuwana, Theodore. Vacuum Heat-Treatment for Activation of Glassy Carbon Electrodes. *Anal. Chem.* **1985**, *57* (14), 2759–2763. <https://doi.org/10.1021/ac00291a006>.
- (21) Zhang, Honghua.; Coury, L. A. Effects of High-Intensity Ultrasound on Glassy Carbon Electrodes. *Anal. Chem.* **1993**, *65* (11), 1552–1558. <https://doi.org/10.1021/ac00059a012>.
- (22) Abdel-Aziz, A. M.; Hassan, H. H.; Badr, I. H. A. Glassy Carbon Electrode Electromodification in the Presence of Organic Monomers: Electropolymerization versus Activation. *Anal. Chem.* **2020**, *92* (11), 7947–7954. <https://doi.org/10.1021/acs.analchem.0c01337>.
- (23) Abdel-Aziz, A. M.; Hassan, H. H.; Badr, I. H. A. Activated Glassy Carbon Electrode as an Electrochemical Sensing Platform for the Determination of 4-Nitrophenol and Dopamine in Real Samples. *ACS Omega* **2022**, *7* (38), 34127–34135. <https://doi.org/10.1021/acsomega.2c03427>.
- (24) Yang, H.-B.; Feceu, A.; Martin, D. B. C. Catalyst-Controlled C–H Functionalization of Adamantanes Using Selective H-Atom Transfer. *ACS Catal* **2019**, *9* (6), 5708–5715. <https://doi.org/10.1021/acscatal.9b01394>.
- (25) Shen, T.; Lambert, T. H. C–H Amination via Electrophotocatalytic Ritter-Type Reaction. *J. Am. Chem. Soc.* **2021**, *143* (23), 8597–8602. <https://doi.org/10.1021/jacs.1c03718>.
- (26) Taily, I. M.; Saha, D.; Banerjee, P. Direct Synthesis of Paracetamol via Site-Selective Electrochemical Ritter-Type C–H Amination of Phenol. *Org. Lett.* **2022**, *24* (12), 2310–2314. <https://doi.org/10.1021/acs.orglett.2c00439>.

